NASA/TM—2010-216941

# Blast Loading of Epoxy Panels Using a Shock Tube

*Mark Pankow and Anthony M. Waas*
*University of Michigan, Ann Arbor, Michigan*

*Brett Bednarcyk*
*Glenn Research Center, Cleveland, Ohio*

December 2010

## NASA STI Program . . . in Profile

Since its founding, NASA has been dedicated to the advancement of aeronautics and space science. The NASA Scientific and Technical Information (STI) program plays a key part in helping NASA maintain this important role.

The NASA STI Program operates under the auspices of the Agency Chief Information Officer. It collects, organizes, provides for archiving, and disseminates NASA's STI. The NASA STI program provides access to the NASA Aeronautics and Space Database and its public interface, the NASA Technical Reports Server, thus providing one of the largest collections of aeronautical and space science STI in the world. Results are published in both non-NASA channels and by NASA in the NASA STI Report Series, which includes the following report types:

- TECHNICAL PUBLICATION. Reports of completed research or a major significant phase of research that present the results of NASA programs and include extensive data or theoretical analysis. Includes compilations of significant scientific and technical data and information deemed to be of continuing reference value. NASA counterpart of peer-reviewed formal professional papers but has less stringent limitations on manuscript length and extent of graphic presentations.

- TECHNICAL MEMORANDUM. Scientific and technical findings that are preliminary or of specialized interest, e.g., quick release reports, working papers, and bibliographies that contain minimal annotation. Does not contain extensive analysis.

- CONTRACTOR REPORT. Scientific and technical findings by NASA-sponsored contractors and grantees.

- CONFERENCE PUBLICATION. Collected papers from scientific and technical conferences, symposia, seminars, or other meetings sponsored or cosponsored by NASA.

- SPECIAL PUBLICATION. Scientific, technical, or historical information from NASA programs, projects, and missions, often concerned with subjects having substantial public interest.

- TECHNICAL TRANSLATION. English-language translations of foreign scientific and technical material pertinent to NASA's mission.

Specialized services also include creating custom thesauri, building customized databases, organizing and publishing research results.

For more information about the NASA STI program, see the following:

- Access the NASA STI program home page at *http://www.sti.nasa.gov*

- E-mail your question via the Internet to *help@sti.nasa.gov*

- Fax your question to the NASA STI Help Desk at 443–757–5803

- Telephone the NASA STI Help Desk at 443–757–5802

- Write to:
  NASA Center for AeroSpace Information (CASI)
  7115 Standard Drive
  Hanover, MD 21076–1320

NASA/TM—2010-216941

# Blast Loading of Epoxy Panels Using a Shock Tube

*Mark Pankow and Anthony M. Waas*
*University of Michigan, Ann Arbor, Michigan*

*Brett Bednarcyk*
*Glenn Research Center, Cleveland, Ohio*

National Aeronautics and
Space Administration

Glenn Research Center
Cleveland, Ohio 44135

December 2010

*Level of Review*: This material has been technically reviewed by technical management.

Available from

NASA Center for Aerospace Information
7115 Standard Drive
Hanover, MD 21076–1320

National Technical Information Service
5301 Shawnee Road
Alexandria, VA 22312

Available electronically at http://gltrs.grc.nasa.gov

# Blast Loading of Epoxy Panels Using a Shock Tube

Mark Pankow and Anthony M. Waas
University of Michigan
Ann Arbor, Michigan 48109–2140

Brett Bednarcyk
National Aeronautics and Space Administration
Glenn Research Center
Cleveland, Ohio 44135

**Abstract**

The high strain rate mechanical response of thin polymer plates has been studied using a modified shock tube. Diagnostics include the pressure-time history of the incident and reflected pulses and the use of digital image correlation (DIC) techniques to extract the time-history of the out-of-plane displacement distribution. Additionally, finite element models have been developed to understand the plate response and to validate and modify plate material constitutive models that have been proposed.

*Key Words: Shock Loading, High Strain rate, Shock Impact, Material Characterization*

---

# 1 Introduction

The study of the response of materials subject to blast loading is imperative to the understanding of how to build blast resistant materials. Until recently the only way to test the materials was through actual blast tests on large size panels, that are costly. However recent developments have used a modification to a shock tube to simulate blast conditions, providing an alternative way to investigate material behavior subjected to blast loading [1].

The shock tube is a well understood instrument, with much of the theory and validation available in the early literature [2]. The corresponding fluid dynamic equations can be found in [3]. In the present work, a modified version of the shock tube is used to understand how a shock wave deforms an initially flat panel. By removing the very thick end cap of the driven tube and replacing it with a relatively thin panel specimen, it becomes possible to subject the panel to a very large pressure pulse acting over a very short-time duration. This method of loading is a very recent development and the literature reflects the novelty of the test at this point [1]. Many of the initial tests conducted using a shock tube were only minimally instrumented and subsequently post-shock tests were conducted to determine the compressive strength or other material property degradation [4, 5]. Additional shock tube tests have been performed on composite plates [6–9], however a lack of data during the deflection and straining of the plate makes it difficult to evaluate the properties and response.

Shock tube studies in conjunction with the development of finite element models have been previously investigated. Initial studies focused on validating an anisotropic damage evolution model for metal plates [10]. Another study attempted to match experimental data of viscoplastic plate vibrations caused by the shock wave impact with finite element simulations [11]. Ultimately the goal would be to blend both problems, i.e that of the shock interaction with the plate response, which becomes a fluid-structure interaction problem. Initial attempts to combine both a fluid dynamics code with a finite element code have been undertaken, with very primitive results [12]. On the other hand if the timescale associated with the shock wave loading is significantly smaller than the plate response time, then the shock loading approximates to a steep pressure step pulse and the ensuing response, if accurately measured, can be used to validate and refine the constitutive models for a variety of rate-dependent materials.

In this paper, results from shock wave loading of epoxy panels are presented. The time-resolved panel response, which is accurately measured using digital image correlation (DIC) techniques, is studied in conjunction with a finite element simulation of the response. This provides a means to validate a rate-dependent constitutive model for the epoxy material.

## 2 Method

Figure 1, shows a schematic of the shock tubes in the Composite Structures Laboratory (CSL) at the University of Michigan. The driver section is loaded with a high pressure gas which is separated from the driven section by a diaphragm designed to burst at a desired driver pressure. When the diaphragm ruptures, a shock wave is formed which travels down the tube at a much faster rate than the pressure can equilibrate. When the shock wave hits the panel specimen, the specimen surface experiences a sudden rise in the pressure and temperature. The shock tube is equipped with pressure transducers (see figure 2), along the driven tube. The pressure transducer mounted on the tube is located 9 in.(0.23 m) from the location of the specimen. The pressure transducers used were made by PCBPiezotronics (model number 113A22) which have a measurement range between 0-5000psi (0-34.5 MPa ) and a resonant frequency greater than 500kHz. They are connected to a 4 channel signal conditioner (model number 482A22). The signal from the signal conditioner then enters the oscilloscope. The driven section always remains at atmospheric pressure.

A complex viewing port system for providing lighting, using flashbulbs, and access for high speed cameras to obtain images to perform the DIC measurements is also present. A schematic of the shock tube hardware incorporating the camera, that was used to obtain the DIC measurements, is shown in figure 3. Prior to testing, the back surface of the specimen is sprayed with a speckle pattern that is suitable for subsequent DIC measurements.

The DIC system provides full-field displacement measurements on the back surface of the panel at pre-selected instances as the deformation progresses. The images are captured using two synchronized Photron SA.1 cameras, that capture images at a rate of one hundred thousand frames per second at a resolution of 320 x 128 pixels. The displacement information can be used to determine the strain components; $\epsilon_X$,$\epsilon_Y$, $\gamma_{XY}$ as a function of position and time on the back surface, and also the time rate of change of these components at different locations on the panel back surface. This is very useful since different areas of the panel experience different levels of strain and rates of straining, depending on the spatial location.

The accuracy of the measurements can be related to the facet size in the DIC software. The resolution of the measurement is $0.16in.(\ 4mm)$. Although the step size is $0.0094in.(0.238mm)$ the size of the computation

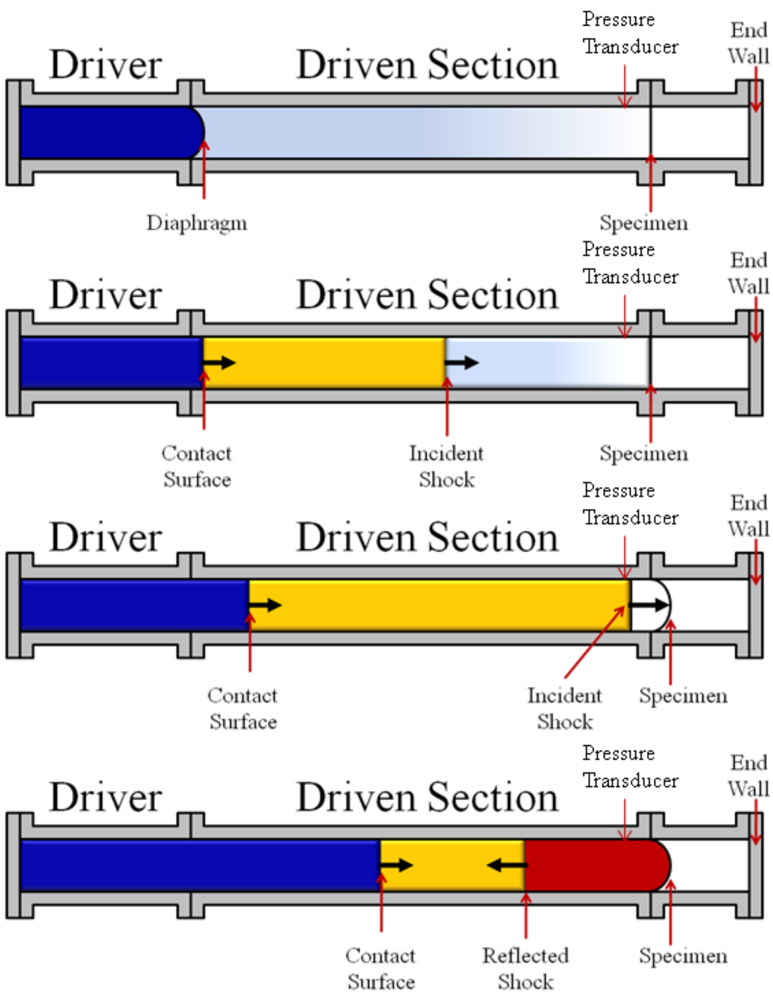


Figure 1: Schematic of the shock tube setup.

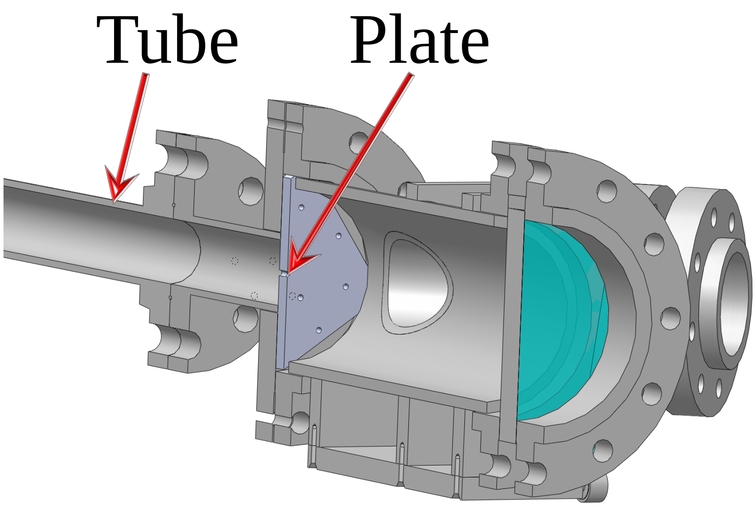


Figure 2: Pressure transducer locations on tube and the plate (specimen).

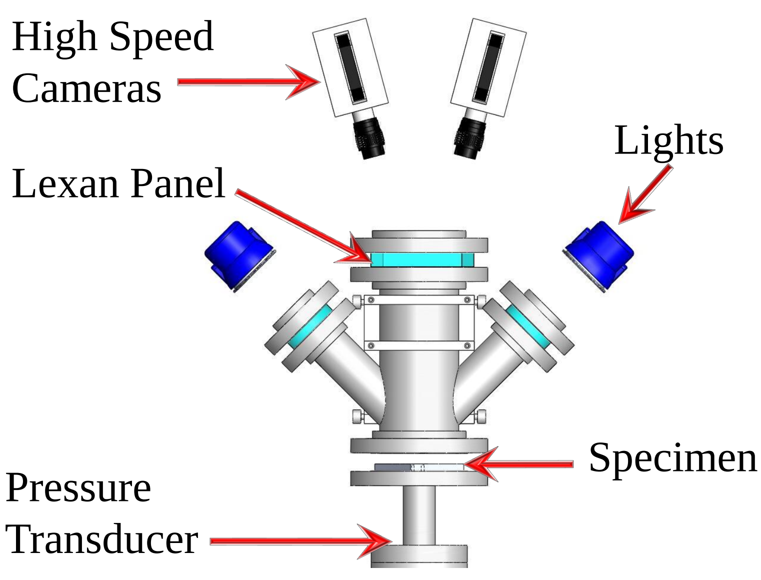


Figure 3: DIC setup for Shock tube Measurements.

box will determine the spatial resolution. The random speckle pattern uses a dot size that is roughly 5-7 pixels in diameter, as recommended by the software manufacturer. The software used in this analysis was ARAMIS, provided by GOM.

The epoxy material was provided to the University of Michigan by NASA Glenn research center. No details on the type of material nor the expected mechanical properties, etc. were provided. It was simply presented as a matrix that would be used in a composite.

Additional tests were performed with a steel plate that was 0.75 in.(19 mm) thick, with mounting holes situated as specified by the manufacturer, at the center, half the radius and edge, to determine the pressure experienced on the surface of the plate. Test results showed that the shock pressure on the plate was uniform, allowing us to assume that the shock wave was normal to the surface.

# 3 Experimental Results

A series of tests were conducted using different thickness epoxy plates. For each thickness test, identical shock tube diaphragms were used so that the burst pressure, and hence the pressure pulse on the specimen, would be nearly the same for materials of the same thickness. The time history of the maximum out-of-plane displacement for a representative test can be seen in figure 4 along with the diaphragm burst pressure. Also indicated is the maximum pressure imposed by the specimen. These results were obtained using the DIC software, and the results of a single frame can be seen in figure 5, which corresponds to a known pressure history of the thickest panel.

In addition to the panel tests performed, another test was run with a "rigid" plate mounted with pressure transducers to record the pressure that was imposed on the impacted plate surface. This pressure-time history is assumed to correspond to those experienced by the epoxy panel specimen. This assumption is valid if the epoxy panel response time is significantly larger than the rise time of the shockwave pressure pulse. The two tests ('rigid' panel and epoxy panel) were performed to experimentally determine the effect of panel deflection on the pressure felt by the panel (i.e. the fluid-structure interaction issue). This information is very important in the subsequent finite element modeling, since one needs to

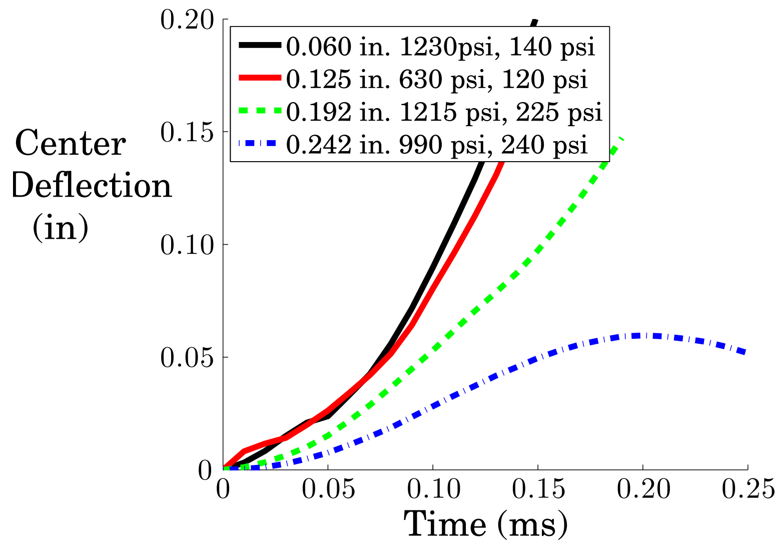


Figure 4: Comparison of maximum out of plane displacement for various specimen thicknesses. The pressure denotes the corresponding diaphragm burst pressure for the test, and the maximum pressure on the specimen.

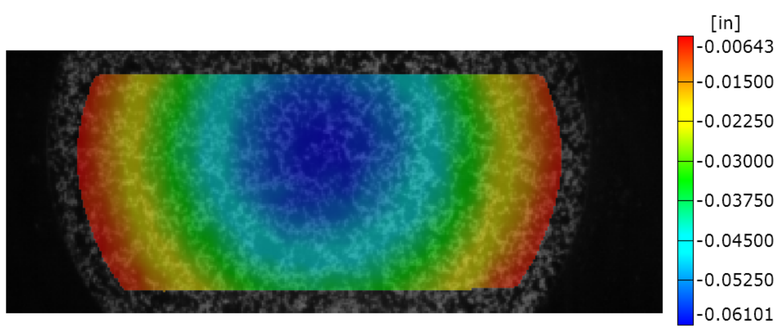


Figure 5: Contour plot of out of plane displacement deformation for a pure epoxy panel.

know the input pressure time-history. Figure 6(a) shows the two pressure-time histories (that have been shifted in time) corresponding to the rigid plate and the thinner epoxy plate as measured. The pressure time history measured on the tube is shown in figure 6(b) along with the pressure measured on the surface of the plate. The results show that the pressure-time histories are very similar, even on the deformable panel. One clear reason for this is the time scales involved in the problem. The pressure pulse increase occurs over a time duration of 0.5 $\mu s$, while the panel deflection, in response to this pressure pulse, occurs over a time duration of 250 $\mu s$, as can be seen in figure 6(c). In summary, the reflected pressure that is measured by the tube pressure transducer can be used as the pressure pulse experienced by the panel specimen. It should be noted that this does not account for fluid-structure interaction that can occur from a rapidly deforming material or interaction with a specimen that fails.

A comparison of the pressure-time history, to the center deflection-time history is shown in figure 6(c). Since the center deflection-time history shows a clear separation in scale, the center plate pressure now appears very similar to a square wave. This result is important in simulations because the shock pulse can be modeled as a square wave to determine what pressure level is needed to induce the desired strains and stresses in a given plate specimen. This calculated pressure can then be related back to a needed burst pressure to produce the required pressure pulse.

With an understanding of the pressure-time histories, the pressure imposed on each panel during testing can be evaluated. The results are shown in table 1 with the corresponding reflected shock pressure being measured from the pressure transducer mounted on the shock tube. The variation in specimen pressure has to do with how the shock wave is reflected off the specimen. If the shock has enough time to compress the specimen the pressure will build however, if the specimen fails or has too great of a deflection, the shock wave will not be completely reflected. Since the thinner specimens failed with larger deflections the strength of the shock wave will not be as strong as if a rigid plate had reflected the shock wave.

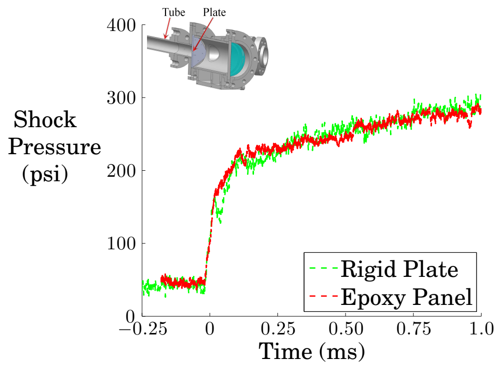


(a) Comparison of tube pressure signals

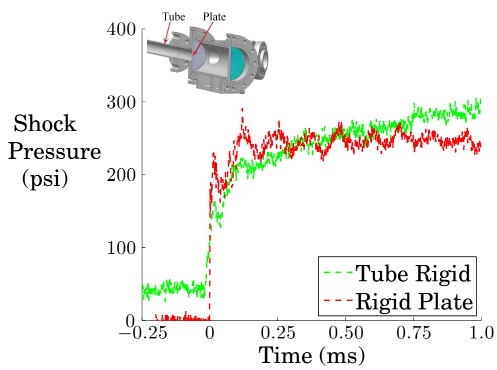


(b) Pressure Transducer in tube vs Pressure transducer on surface of rigid plate

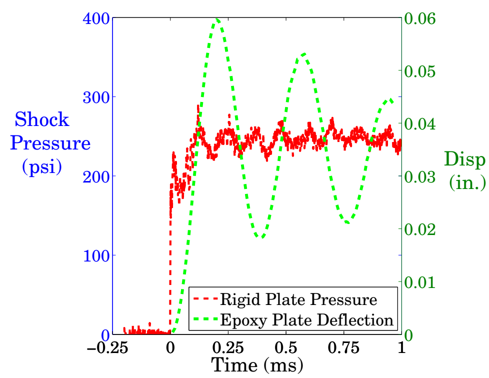


(c) Pressure on rigid plate and center deflection of epoxy panel

Figure 6: Pressure-time histories and center deflection (Epoxy Panel) of shock tube test. Time has been shifted to show relative data comparison.

Table 1: Burst and shock pressures for various thicknesses.

| Thickness (in.) | Diaphragm Burst Pressure (psi) | Shock Pressure (psi) |
|---|---|---|
| 0.060 | 1230 | 140 |
| 0.125 | 630 | 120 |
| 0.192 | 1215 | 225 |
| 0.242 | 990 | 240 |

# 4 Computational Model

A finite element (FE) model was developed to understand the pulse-loaded panel response. Initially, a homogeneous isotropic plate model using non-linear geometry was created in ABAQUS version 6.8, to simulate the epoxy panel response, using an explicit solver. The measured pressure-time history is used as a "square wave" input loading. This assumption does not allow for fluid-structure interaction and the propagation of further shock waves. The epoxy material was modeled using J2 small strain theory of plasticity with isotropic hardening and a von Mises yield criterion, where the material properties are to be determined through inverse modeling, by correlation with the test data. A circular 3 inch specimen corresponding to the specimen dimensions used in the shock tests, was analyzed using the FE method. The panel mesh contains 458 elements with 254 nodes, with S3R shell elements being used. The mesh size was determined using a convergence study, the results of which are shown in figure 7

For materials which have a rate-independent modulus the Cowper-Symonds overstress power law is used to approximate the effects of strain rate on yield stress.

$$\dot{\epsilon}^{pl} = D(R-1)^n, \tag{1}$$

where $D$ and $n$ are material constants and $R$ is the yield stress ratio, $\frac{\sigma}{\sigma_0}$. Since the rate dependence of the epoxy is an unknown, an initial attempt was made using the rate-dependent properties of a similar polymer ma-

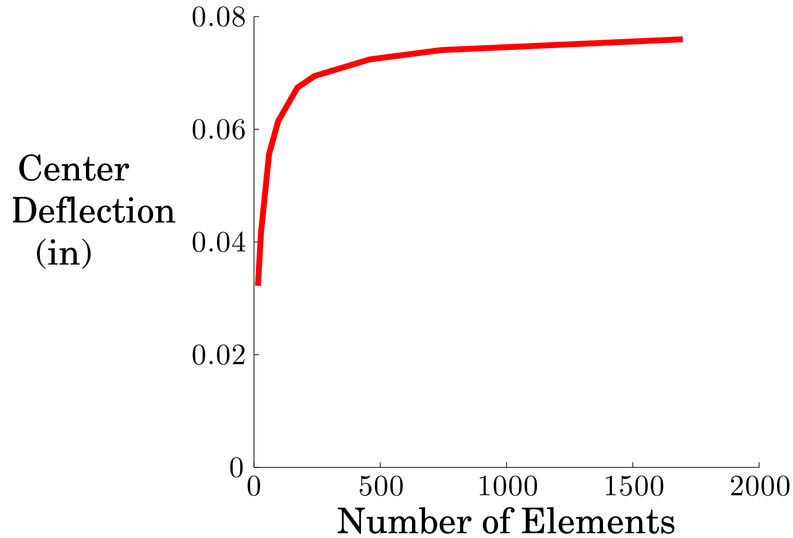


Figure 7: Finite Element Convergence Study

terial. Split Hopkinson pressure bar test results for the rate dependence of SC-15, a thermoset polymer matrix material, were used as a guide for an ”initial guess” of the rate-dependent properties. SC-15 epoxy is a low-viscosity, two-phased toughened epoxy resin system consisting of phase A (resin mixture of diglycidylether epoxy toughener) and phase B (hardener mixture of cycloaliphaic amine poluoxylalkylamine) [13]. The assumed rate dependence for SC-15 is plotted as a solid line in figure 8, where the circles represent the experimental data.

Due to the complexity of the constitutive model many parameters need to be determined; these are, modulus, yield stress ratio, power law exponent, and material damping. The known inputs can be seen in table 2. In a brittle epoxy sample, a test that subjects the panel to failure provides very little information about the yield and plasticity parameters. From such a test, about all that can be determined are the initial modulus and failure strength. Therefore, if a panel test is conducted at a suitable burst pressure below the plate to fracture level, the resulting oscillatory out-of-plane panel response provides information that can be used to determine several of the material parameters.

Through the use of inverse modeling the following parameters for the

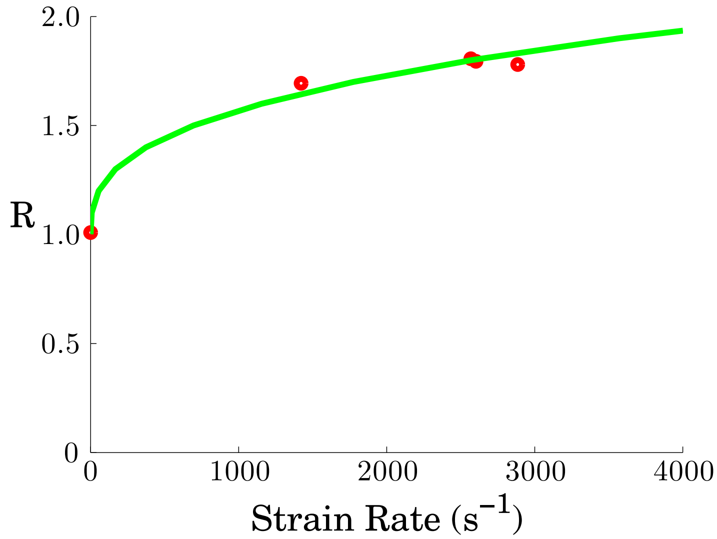


Figure 8: $\dot{\epsilon}$ vs. $\frac{\sigma}{\sigma_0}$ for SC-15 Matrix

Table 2: Sample Test Known Parameters

| | | |
|---|---|---|
| Thickness | 0.242 | in. |
| Density | $1.14e-4$ | $\frac{lbs}{in^3}$ |

epoxy material have been determined (see table 3), by matching the time history of events. With the use of the parameters shown in table 3, a comparison between experiment and simulation for the panel out-of-plane deflection can be made and is shown in figure 9. A consistent error between the computed and measured displacement amplitude history is seen, even though the frequency of response is matched almost exactly. Reviewing the hardware configuration of the DIC system, it becomes apparent that an inherent error was inadvertently introduced into the system. Figure 10 shows that the optical path can shift, due to any shift in the position of the lexan panel window, causing a parallax error. When the system was initially calibrated the containment chamber was a distance 'd' away from the mount. However when the tests were run 'd' became zero as the system was clamped together. The cameras remained at the same fixed

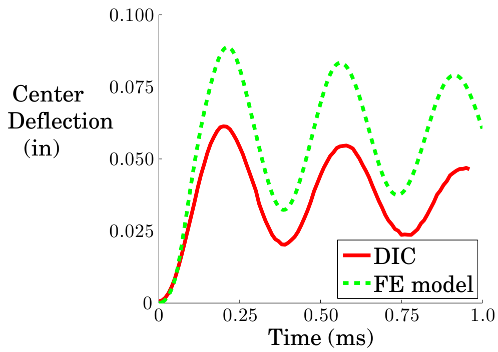


Figure 9: Finite Element Results vs. DIC results

distance from the point where the specimen is mounted. This shift will cause a change in the DIC systems measurements since the optical path shift introduces a systematic error into the initial image calibration. When the DIC system is initially calibrated, the distance 'd' must be held at the same value to be used later during the actual tests. Additional error could have been introduced if the assumed material properties from the SC-15 data were inaccurate, since only one run was used to curve fit many different properties.

Table 3: Sample Test Parameters

| | | |
|---|---|---|
| Modulus | $350,000$ | $\frac{lbs}{in^2}$ |
| $\sigma_y$ | $3,250$ | $\frac{lbs}{in^2}$ |
| D | 4880 | |
| n | 2.883 | |

In addition to displacements, the strain histories are also compared. Since strains are based on displacement data there will again be a mismatch due to the parallax error in terms of magnitude however, the general trend and contours should be the same. The results compare a section line through the center in the DIC results, which are seen in figures 11 and 12. There is an excellent agreement between the FE predicted result and the DIC extracted result. The values of $\epsilon_{xx}$ show nearly identical con-

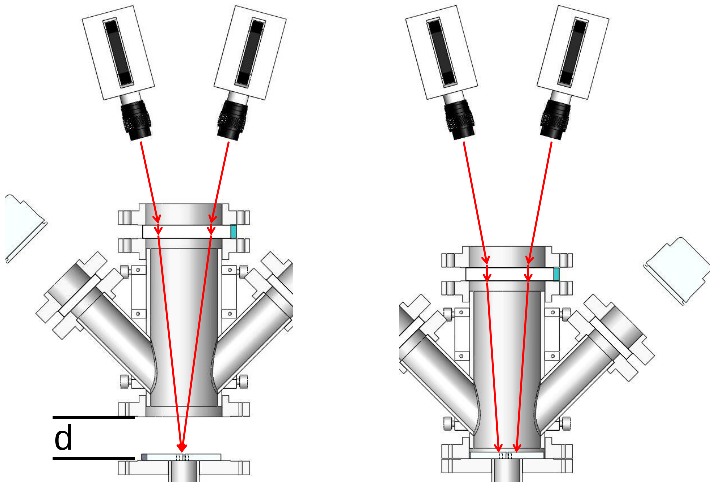


Figure 10: Difference in optical paths from movement of lexan panel.

tour maps which is due to very little out-of-plane displacement $0.06in.$ occurred relative to the overall size of the specimen $3in.$ therefore, the calculations for strains becomes more reliant on the 2D motion, which can be captured accurately with 1 camera. The DIC results show that there is some localized strain effects, which could be caused by imperfections in the material.

With a focus on strain rate dependent material properties, a representative point in the center of the panel is examined. The center of the panel produces a biaxial stress state, which implies that both $\epsilon_{xx}$ and $\epsilon_{yy}$ are the same value for an isotropic material. The strain-time history for the center point can be seen in figure 13. As can be seen there is very good agreement between the two results. From the strain-time histories, the strain rates are computed and shown in figure 14. As can be seen in figure 13, there is a considerable amount of noise in the DIC data. The data was filtered, using a ninth order polynomial curve fit, to eliminate much of the noise so that one can observe a general trend. There is an initial peak followed by a spiral pattern as the plate oscillates. To better see this, the strain components at the center, as predicted from the finite element simulation, are shown in figure 15. This plot shows that we have attained a medium strain rate (50-200 $\frac{1}{s}$, see figure 14) for the material. We have not achieved an ultra-

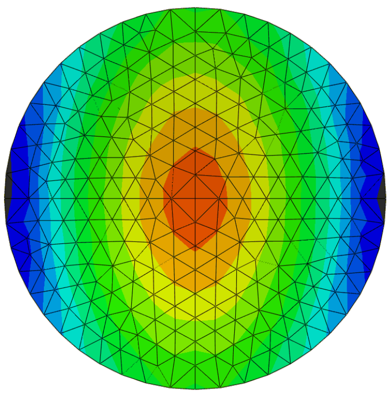

(a) Finite Element

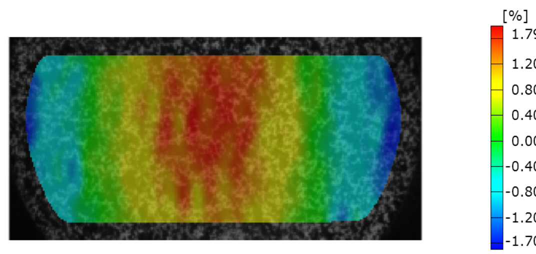


(b) DIC

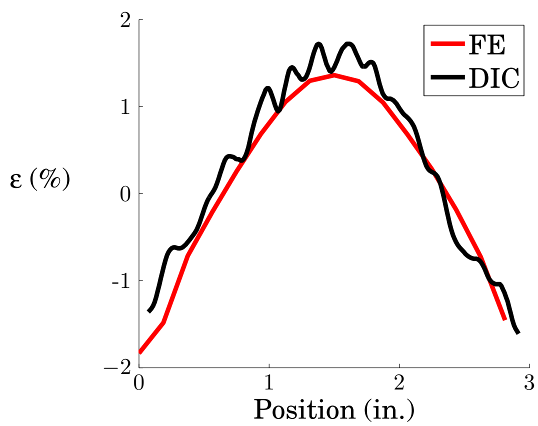


(c) Section Line

Figure 11: Comparison of $\epsilon_{xx}$ results at max displacement.

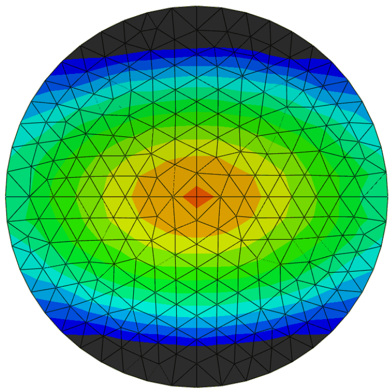

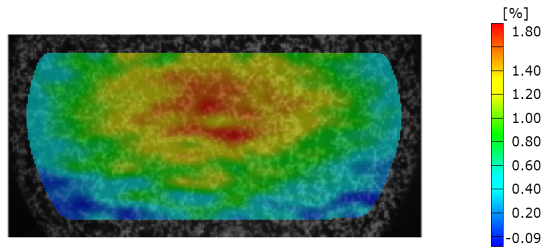


(a) Finite Element (b) DIC

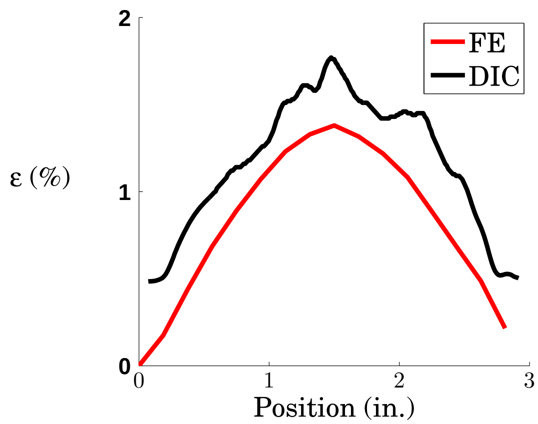


(c) Section Line

Figure 12: Comparison of $\epsilon_{yy}$ results at max displacement.

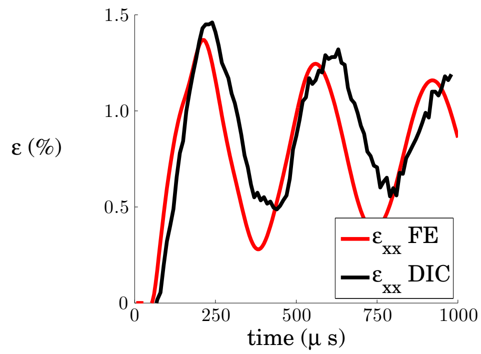


Figure 13: Strain time history of center point comparing FE vs. DIC

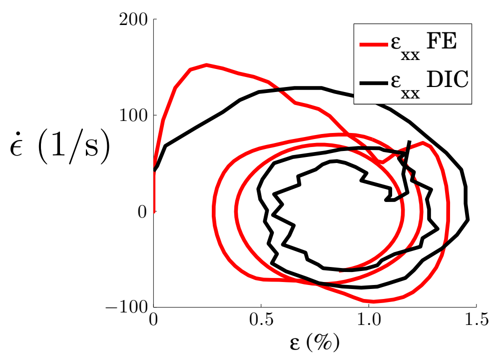


Figure 14: Strain rate vs. strain history at the crown of the panel; comparison between the FE model and DIC results, which have been filtered.

high rate (2000-3000 $\frac{1}{s}$, see figure 8) as seen in the Hopkinson bar. The material will have ranges of constant strain rate and also oscillate about this strain rate. Figure 14 shows how the material will respond to a strain rate of $100\frac{1}{s}$ staying relatively constant until it reaches a maximum strain, reversing and going to a strain rate of $-75\frac{1}{s}$, and then as the oscillations continue it will return to $75\frac{1}{s}$ and shift to $-75\frac{1}{s}$ as the deflection decreases. From figure 15 it is observed that the shear strain is negligible, since its values and contributions are less than 1% of $\epsilon_x$ and $\epsilon_y$.

The remaining test results (where the panel fractured) were used to determine the stress level when failure occurred. Since this material is very brittle at high strain rates, there is minimal yielding. The test results were

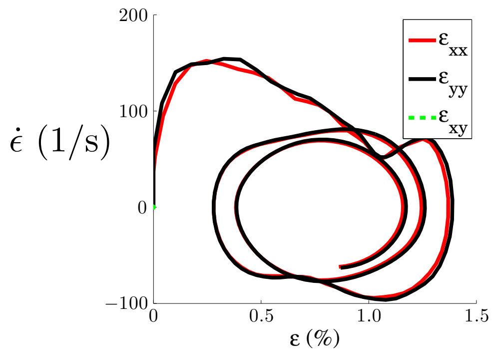


Figure 15: Strain rate vs. strain history at the crown of the panel from FE model.

compared to properties determined by the FE simulation model and used to back out the failure stress, based on the time that failure was recorded with the Photron cameras. It should be noted that the model is based on SHPB data from a separate material, along with the fact that the data was collected at much higher strain rates. Additionally, the different thickness of materials may have different material properties, based upon slight processing variations. Therefore, the model should only be used to note trends.

A summary of the computed failure stresses, and the out-of-plane deflections, as a function of panel thickness, is provided in table 4. Here the failure stress is produced from the FE model and the displacement and failure time are obtained from the DIC software. It is seen that at the very high rates, panel failure occurs in the brittle-elastic regime, as was evident in the failure mode of the material and the small amount of plasticity measured in the model.

# 5 Conclusion

A methodology has been developed to determine the mechanical response of materials subjected to pressure pulse loading. Using high speed cameras, the out-of-plane deflection time history has been measured using the DIC method. This result, in conjunction with a finite element model and Hopkinson bar data can be used to inverse model the panel response and

Table 4: Failure Stress

| Thickness (in.) | Failure Stress (psi) | Time ($\mu s$) | Z-Disp (in.) |
|---|---|---|---|
| 0.060 | 7,635 | 120 | 0.152 |
| 0.125 | 6,860 | 120 | 0.131 |
| 0.192 | 6,599 | 130 | 0.0874 |
| 0.242 | 5,421 | 130 | 0.0587 |

validate the rate-dependent properties of the panel. The pressure-time history is used as an input to the finite element simulation. It has been shown that the pressure transducer closest to the panel on the driven tube provides information regarding the loading of the specimen. In the shock tube tests, it is beneficial to stop the testing prior to failure, rather than having an oscillatory panel response, since that allows the determination of a larger number of material parameters. Tests to failure provide additional information on rate-dependent material strength and mode of failure.

# References


[1] M. Stoffel. Measurement technique for shock wave-loaded structures and its applications. *Experimental Mechanics*, 46:47–55, 2006.

[2] H.W. Liepmann and A. Roshko. *Elements of Gasdynamics*. Wiley, 1957.

[3] J.D. Anderson. *Modern Compressible Flow*. McGraw-Hill, 3rd edition, 2002.

[4] J. LeBlanc, A. Shukla, C. Rousseau, and A. Bogdanovich. Shock loading of three-dimensional woven composite materials. *Composite Structures*, 79:344–355, 2007.

[5] M. Herbert, C.E. Rousseau, and A. Shukla. Shock loading and drop weight impact response of glass reinforced polymer composites. *Composite Structures*, 84:199–208, 2008.

[6] S.A. Tekalur, A. Shukla, and K. Shivakumar. Blast resistance of polyurea based layered composite materials. *Composite Structures*, 84:271–281, 2008.

[7] S.A. Tekalur, K. Shivakumar, and A. Shukla. Mechanical behavior and damage evolution in e-glass vinyl ester and carbon composites subjected to static and blast loads. *Composites Part B: Engineering*, 39:57–65, 2008.

[8] S.A. Tekalur, A.E. Bogdanovich, and A. Shukla. Shock loading response of sandwich panels with 3-d woven e-glass composite skinds and stitched foam core. *Composite Science and Technology*, 6:736–753, 2009.

[9] Q. Li, D. Liu, D. Templeton, and B. Raju. A shock tube-based facility for impact testing. *Experimental Techniques*, (25–28), 2007.

[10] M. Stoffel. Experimental validation of anisotropic ductile damage and failure of shock wave-loaded plates. *European Journal of Mechanics A/Solids*, 26:592–610, 2007.

[11] M. Stoffel, R. Schmidt, and D. Weichert. Shock wave-loaded plates. *International Journal of Solids and Structures*, 38:7659–7680, 2001.

[12] M. Gong and Y. Andreopoulos. Shock wave impact on monolithic and composite material plates: The preferential aeroelastic response. *Journal of Sound and Vibration*, 313:171–194, 2008.

[13] Y. Zhou, F. Pervin, M.A. Biswas, V.K. Rangari, and S. Jeelani. Fabrication and characterization of montmorillonite clay-filled sc-15 epoxy. *Materials letters*, 60:869–873, 2006.

| REPORT DOCUMENTATION PAGE | | *Form Approved OMB No. 0704-0188* |
|---|---|---|



**1. REPORT DATE** *(DD-MM-YYYY)*
01-12-2010

**2. REPORT TYPE**
Technical Memorandum

**3. DATES COVERED** *(From - To)*

**4. TITLE AND SUBTITLE**
Blast Loading of Epoxy Panels Using a Shock Tube

**5a. CONTRACT NUMBER**

**5b. GRANT NUMBER**

**5c. PROGRAM ELEMENT NUMBER**

**6. AUTHOR(S)**
Pankow, Mark; Waas, Anthony, M.; Bednarcyk, Brett

**5d. PROJECT NUMBER**

**5e. TASK NUMBER**

**5f. WORK UNIT NUMBER**
WBS 698259.02.07.03

**7. PERFORMING ORGANIZATION NAME(S) AND ADDRESS(ES)**
National Aeronautics and Space Administration
John H. Glenn Research Center at Lewis Field
Cleveland, Ohio 44135-3191

**8. PERFORMING ORGANIZATION REPORT NUMBER**
E-17545

**9. SPONSORING/MONITORING AGENCY NAME(S) AND ADDRESS(ES)**
National Aeronautics and Space Administration
Washington, DC 20546-0001

**10. SPONSORING/MONITOR'S ACRONYM(S)**
NASA

**11. SPONSORING/MONITORING REPORT NUMBER**
NASA/TM-2010-216941

**12. DISTRIBUTION/AVAILABILITY STATEMENT**
Unclassified-Unlimited
Subject Category: 39
Available electronically at http://gltrs.grc.nasa.gov
This publication is available from the NASA Center for AeroSpace Information, 443-757-5802

**13. SUPPLEMENTARY NOTES**

**14. ABSTRACT**
The high strain rate mechanical response of thin polymer plates has been studied using a modified shock tube. Diagnostics include the pressure-time history of the incident and reflected pulses and the use of digital image correlation (DIC) techniques to extract the time-history of the out-of-plane displacement distribution. Additionally, finite element models have been developed to understand the plate response and to validate and modify plate material constitutive models that have been proposed.

**15. SUBJECT TERMS**
Strain rate; Thin plates; Shock tubes; Imaging techniques; Displacement; Finite element method; Characterization

| 16. SECURITY CLASSIFICATION OF: a. REPORT | b. ABSTRACT | c. THIS PAGE | 17. LIMITATION OF ABSTRACT | 18. NUMBER OF PAGES | 19a. NAME OF RESPONSIBLE PERSON |
|---|---|---|---|---|---|
| U | U | U | UU | 26 | STI Help Desk (email:help@sti.nasa.gov) |
| | | | | | **19b. TELEPHONE NUMBER** *(include area code)* 443-757-5802 |